Available online at www.sciencedirect.com
ScienceDirect
International Journal of Pharmaceutics 339 (2007) 91–102
INTERNATIONAL JOURNAL OF PHARMACEUTICS
www.elsevier.com/locate/ijpharm

Combinatorial design of passive drug delivery platforms

Sébastien Casault, Martin Kenward, Gary W. Slater *

Department of Physics, University of Ottawa, 150 Louis-Pasteur, Ottawa, Ontario K1N 6N5, Canada

Received 19 December 2006; received in revised form 22 February 2007; accepted 22 February 2007
Available online 1 March 2007

Abstract

We introduce a novel computational approach to designing passive drug delivery systems based on porous materials such as hydrogels. Our approach uses three tools: a method to establish the exact release pattern from all possible loading sites inside a given hydrogel; a method to generate a large number of hydrogel structures to be tested numerically, and finally an optimization algorithm which leads to the selection of optimal hydrogel structures. Using this approach, we show that controlled release curves can be obtained by using a genetic algorithm for the optimization step. Strategies to generalize this approach to other systems are also discussed.

Keywords: Drug delivery; Controlled release; Hydrogels; Optimization; Genetic algorithm; Exact-enumeration

1. Introduction

Designing drug delivery systems with a controlled rate of drug release is crucial for applications where dosage must remain in a prescribed therapeutic range over the entire term of treatment (Peppas and Langer, 1994). Currently, there exists activation modulated platforms relying on kinematic effects (e.g., swelling and dissolution) that feature controlled release characteristics (Saltzman and Olbricht, 2002; Mallapragada et al., 1997). However, it proves much more challenging to achieve constant drug release from passive platforms, i.e., those strictly relying on diffusion as a drug delivery mechanism, such as non-degradable hydrogels (Conaghey et al., 1998; Liu et al., 2003). Passive platforms would have the advantage of not heavily relying on environmental factors which can prove difficult to control. There is a definite need for a systematic approach which can quickly identify optimal design strategies for passive systems.

According to Cohen and Erneux (1998), the most common drug delivery mechanism is diffusion from a polymeric system (such as a hydrogel). We will thus focus our study on hydrophilic drugs escaping from non-swelling diffusion-controlled hydrogels. Since this is the most widely applicable release mechanism (Lin and Metters, 2006), several methods can be used experimentally to prepare hydrogels with specific internal structures (obstacle distributions). For example, Liang et al. (2003) have shown that the density of a hydrogel can be controlled using a non-cytotoxic crosslinker.

We introduce the novel concept of combinatorial drug delivery platform design. This technique is used to investigate hydrogel structures which exhibit specific release characteristics. We focus this proof of principle study on obtaining results which promote a constant drug release rate as a function of time although the technique can be used, in principle, to achieve virtually any desired release profile. The results presented in this paper are obtained using a lattice model of diffusion which is similar to that introduced originally by Majid et al. (1984). We neglect chemical details and adopt a coarse-grained view of the diffusion process. Studies which model polymers often rely on stochastic, Monte Carlo simulation methods where the diffusion of a drug molecule is represented by random, discrete jumps on a lattice occupied with obstacles. In contrast, our method has the advantage of producing numerically exact data by enumerating all possible walks on any given lattice matrix with obstacles (the latter represent the gel fibers present in a hydrogel matrix). We limit our work to diffusion in two-dimensions but the extension to 3D (or more!) poses no difficulty other than requiring more computational resources.

It is widely known that the internal structure of a hydrogel is important in modulating the release rate (Kosmidis et al., 2003; Bunde et al., 1985; Hastedt and Wright, 1990; Amsden, 1998; Siepmann and Peppas, 2001). Constructing hydrogels with specific structures and testing their drug release properties

* Corresponding author.
E-mail address: gary.slater@uottawa.ca (G.W. Slater).

0378-5173/$ – see front matter © 2007 Elsevier B.V. All rights reserved.
doi:10.1016/j.ijpharm.2007.02.029

is experimentally time consuming. Using our method, we can reduce the amount of experiments needed by offering critical information on how to tailor the structure of a hydrogel in order to obtain specific release profiles. Although the structure of the hydrogel is important, the initial loading of the drug itself inside the structure is equally critical. Accordingly, we will also use our optimization technique to investigate the placement of drug reservoirs inside the hydrogel.

It is also possible to obtain numerically exact values of the diffusion coefficient for practically any hydrogel structure (Mercier and Slater, 1999a,b; Nieuwenhuizen et al., 1986). However, the diffusion coefficient is not always the key factor in predicting the release characteristics of complex systems (e.g., one must also consider the geometry and dimensionality of the hydrogel). For this reason, we use the exact enumeration model mentioned earlier which makes no assumption about the functional form of the diffusion coefficient. This numerically exact lattice calculation of the short-time diffusion dynamics of a particle is much quicker to perform than Monte Carlo simulations. This method essentially consists in finding the transfer matrix for any given obstacle configuration and their relative positions as a function of time. Thus, any minor change to either will equate to changing a single row in the transfer matrix and thus can be recomputed fairly easily. This allows one to very quickly perform changes in the initial conditions (e.g., modifying the obstacle pattern) and measure the resulting escape rates. Using a genetic algorithm as our optimization tool, it is then possible to study several thousand combinations of (evolving) hydrogel structures in order to rank them according to their usefulness in generating desired release rates.

This article is structured as follows: we begin by presenting the theory of the enumeration method followed by examples to test its validity. The optimization technique used throughout this paper is then presented. Finally, we present results obtained using our technique for drug delivery systems with different geometries.

2. Enumeration methodology

2.1. Diffusion model

Enumeration methods allow one to obtain exact numerical results for problems related to diffusion, escape rates and transient effects (Majid et al., 1984). To illustrate this, let us first examine diffusion on a simple 2D square lattice (Fig. 1). We compute all possible particle trajectories of a solute, based on its initial location and its probability to diffuse to any first nearest neighbour on the lattice. Fig. 1 shows the evolution through three time steps of solute diffusion on a typical 2D square lattice with three obstacles.

The probability to diffuse in any given Cartesian direction is simply $p_{\pm x} = p_{\pm y} = 1/4$. In an isotropic system, a given solute particle has an equal probability to diffuse (or jump) to any four of the nearest neighbour sites. Time is discrete and all particles must attempt a jump at each time step. A move is simply rejected (i.e., the particle is reflected) if the neighbouring site is occupied by an obstacle. In other words, we assume elastic collisions.

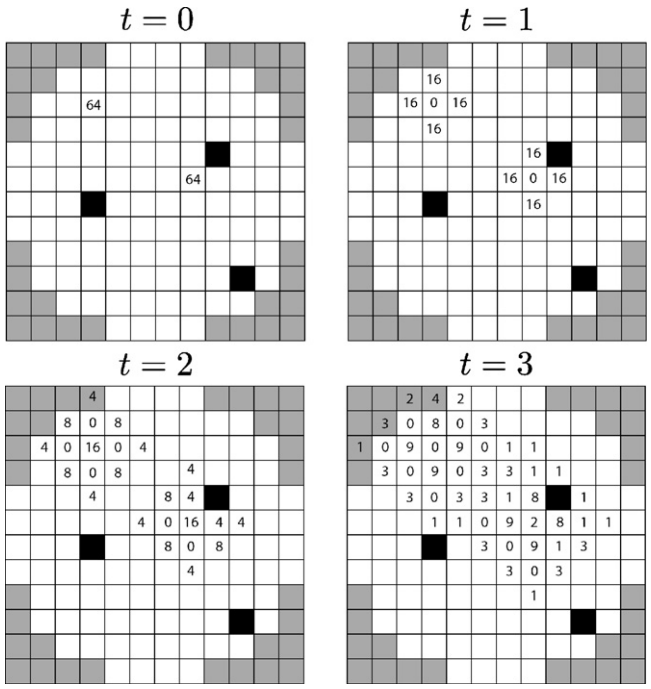

Fig. 1. Time evolution of a typical circular system with particles undergoing diffusion on a 2D square matrix with three obstacles (black). The absorbing boundary is shown in grey (the sides are also part of this boundary). The initial configuration is shown at $t = 0$ with the drug molecules completely localized on two sites.

Lattices with higher coordination numbers such as the hexagonal lattice were considered for this model; however they lead to prohibitively long computational times and marginal differences in release profiles.

A uniform probability of jumping is valid as long as there is no drug-hydrogel affinity, external field or other source of anisotropy. For example, in a real system the drug may exhibit affinity for the obstacles. This could be implemented by adding a probability p_o for the particle to stay on the same site when it is next to a "sticky" obstacle.

In the current study, obstacles are completely passive and do not respond to temperature variations or external effects (varying pH, electric fields, etc.). Also, the obstacle density is time-independent, i.e., there are no degradation or swelling effects. Such active parameters would require major changes to the method introduced in this article since they generally involve a non-deterministic evolution of the hydrogel matrix.

The general two-dimensional master equation governing the probability of having a drug concentration $C_{x,y}(t)$ on a free site at (x, y) at time t is:

$$\begin{aligned} C_{x,y}(t+1) = {} & [C_{x-1,y}(t)(1 - q_{x-1,y}) + C_{x,y}(t)q_{x+1,y}]p_{+x} \\ & + [C_{x+1,y}(t)(1 - q_{x+1,y}) + C_{x,y}(t)q_{x-1,y}]p_{-x} \\ & + [C_{x,y-1}(t)(1 - q_{x,y-1}) + C_{x,y}(t)q_{x,y+1}]p_{+y} \\ & + [C_{x,y+1}(t)(1 - q_{x,y+1}) + C_{x,y}(t)q_{x,y-1}]p_{-y}. \end{aligned} \quad (1)$$

In this equation, $q_{x,y}$ is the site occupation index; its value is 1 if the site at (x, y) is occupied by an obstacle and 0 if not. Note that for a given system, the value of $q_{x,y}$ is fixed for all lattice sites and is simply determined by the structure of the hydrogel. As schematically illustrated in Fig. 1, the calculation is done iteratively, from an initial drug concentration $C_{x,y}(0)$ for each site on the lattice. We make the assumption that we are in the low drug concentration (dilute) regime where solute particles do not interact with each other.

In order to model drug release from a finite-sized hydrogel system, one simply imposes absorbing boundary conditions $p_{\pm x} = p_{\pm y} = 0$ on the outer boundary of the hydrogel structure. The amount of drug crossing this boundary is the cumulative sum of all those probabilities which have crossed the boundary up to time t.

In this paper, we restrict our work to examine simple cases which do not include surface kinetic effects. Nevertheless it is straightforward to tailor the surface properties of our simulated drug delivery system to reflect conditions which may arise from certain hydrogel/solute/environment configurations (e.g., resistance to escape at the boundary, pH or viscosity gradients at the surface of the hydrogel, etc.).

If the various local concentrations $C_{x,y}(t)$ (including those in the absorbing layer) are grouped into a column vector $|C(t)\rangle$ with s elements (one for each lattice site; note that we use Dirac's bra-ket notation), Eq. (1) can be rewritten as a matrix equation

$$|C(t+1)\rangle = \mathbf{T}|C(t)\rangle. \tag{2}$$

The $s \times s$ Markovian matrix $\mathbf{T}$ (which depends entirely on the positions of the obstacles) transforms the distribution at time t into the one at time $t+1$. This provides a simple computational method to carry out the iterations that are implicit in Eq. (1) starting from an initial drug load $|C(0)\rangle$. Mathematically, it is possible to use this equation backwards, i.e., start with a given final release rate and calculate the corresponding initial configuration. This unfortunately yields unrealistic parameters (e.g., negative initial concentrations in certain regions) and is not useful in practice.

Using this exact enumeration method, we calculate the associated release rate curves. Our goal is to find an initial capsule configuration (which is defined by the obstacle locations $\mathbf{T}$ and drug loading $|C(0)\rangle$) which yields a desired release rate, e.g., a constant release rate for long time periods.

2.2. Notation

For the sake of clarity, we introduce the notation $M(t)$ to indicate the total drug released as a function of time:

$$M(t) = M_0 - \int_0^t \int_\Omega C(\vec{r}, t')\, \mathrm{d}\Omega\, \mathrm{d}t' \tag{3}$$

where

$$M_0 = \int_\Omega C(\vec{r}, 0)\, \mathrm{d}\Omega \tag{4}$$

represents the total initial amount of drugs present in a hydrogel. $C(\vec{r}, t')$ describes the drug concentration at position $\vec{r}$ at time t' and Ω represents the area (or volume for three-dimensional simulations) of the hydrogel. One can write $\tilde{M}(t)$ as the normalized cumulative amount of drugs released at time t

$$\tilde{M}(t) = \frac{M(t)}{M_0}. \tag{5}$$

One can define an asymptotic release amount $M(\infty)$ (it is equal to the M_0 if no drug particle is trapped inside the hydrogel). Also, we introduce the parameter τ_ϕ which we define as the time at which a certain fraction, ϕ, of drugs has been released from the system

$$\phi = \frac{M(\tau_\phi)}{M_0}. \tag{6}$$

Finally, the rate of drug release is measured by the derivative

$$\dot{M} = \frac{\partial M}{\partial t}. \tag{7}$$

Similarly, one can define a normalized rate $\dot{\tilde{M}}(t)$.

2.3. Uniformly loaded gels: empirical fits

A uniformly loaded gel is defined as having an equal concentration of solute on every non-obstacle site; drug is said to be uniformly loaded in the hydrogel matrix. There is no lag time (i.e., time lapse between the beginning of the enumeration and the arrival of the effective drug concentration "wavefront" at the boundary) in this scheme since there is a drug concentration near the boundary which escapes the hydrogel at $t = 1$. We later show that optimization of the hydrogel matrix can be related to this lag time and that schemes involving drug reservoirs that are non-adjacent to the boundary can be of crucial importance when searching for a constant rate of release.

We can simulate such a uniformly loaded hydrogel and compare our numerical data with two widely used empirical fits. According to Peppas (1985), a simple power-law relationship can describe the time dependence of drug release until 60% of the initial load has been released:

$$\tilde{M}(t) = \left(\frac{t}{t_\alpha}\right)^\alpha \tag{8}$$

where α is the release exponent, and the resulting time scale t_α is relevant only for short times ($\tilde{M} \ll 1$). Since the Peppas equation is not bounded as $t \to \infty$ it cannot be used to model the escape at long times.

According to a more general statistical theory, the Weibull model predicts that the release rate behaves like a stretched exponential (Weibull, 1951):

$$\tilde{M}(t) = 1 - \exp\left[-\left(\frac{t}{t_\beta}\right)^\beta\right]. \tag{9}$$

The parameters are now the exponent, β and the time scale t_β. A series expansion of the Weibull function yields the Peppas law to first order and thus it is expected that $\beta \to \alpha$ and $t_\beta \to t_\alpha$ as $t \to 0$. However, both these empirical fits suffer from an apparent lack of physical meaning associated with the free parameters.

2.4. Exact solution for a test system

It is possible to solve the 2D diffusion equation in polar coordinates for $C(r,t)$ to obtain a predicted release curve from a round hydrogel with radius r_0 (Crank, 1975) and uniform drug concentration. In this case, we simply replace the obstacles inside the capsule by an effective viscosity (or, more precisely, by an effective diffusion coefficient D^*) which models the retarded diffusive motion of the particles. Since the distribution of obstacles is assumed to be isotropic, D^* is simply a fitting parameter.

We study here a circular drug capsule with an isotropic obstacle distribution with a concentration well bellow the percolation threshold, $\mathcal{C}^*_{\text{obst}}$ ($\mathcal{C}^*_{\text{obst}} \simeq 0.408$ for a square lattice (Reynolds et al., 1980)). The capsule is said to be uniformly loaded, i.e., an equal drug concentration occupies every non-obstacle site. The 2D diffusion equation in polar coordinates can be written as

$$\frac{\partial C(r,t)}{\partial t} = D^* \left(\frac{\partial^2}{\partial r^2} + \frac{1}{r}\frac{\partial}{\partial r} \right) C(r,t) \tag{10}$$

with boundary conditions

$$C(r,0) = \mathcal{H}(r - r_0)C_0 \tag{11a}$$

$$C(r_0,t) = 0, \tag{11b}$$

where $\mathcal{H}$ is the heaviside function, and C_0 is the initial drug concentration of the free sites inside the capsule. Eq. (11b) accounts for the absorbing boundary. The solution to Eq. (10) is given by the following:

$$C(r',t) = \sum_{n=1}^{\infty} C_n(r_0) J_0(\lambda_n r') \exp\left[-D^* \left(\frac{\lambda_n}{r_0} \right)^2 t \right] \tag{12}$$

where J_0 is the 0th order Bessel function of the first kind, λ_n represents the nth zero of $J_0(r)$, $r' = r/r_0$ is a scaled radial position, and the coefficients, $C_n(r_0)$, are given by:

$$C_n(r_0) = \frac{2C_0}{J_1^2(\lambda_n)} \int_0^1 \mathcal{H}(r - r_0) J_0(\lambda_n r') r' \, \mathrm{d}r'. \tag{13}$$

Table 1 shows the first four $C_n(r_0)$ coefficients in the series solution to the diffusion equation. In the next two sections, we will compare our exact enumeration results to the Peppas and Weibull empirical fits as well as to this exact solution based on the existence of an effective diffusion coefficient D^* for the given system.

Table 1
The first four λ values and the corresponding $C_n(r_0)$ coefficients used in the diffusion equation with $r_0 = 1$

n	λ_n	$C_n(r_0)$
1	2.4048	1.6020
2	5.5201	−1.0648
3	8.6537	0.8514
4	11.7915	−0.7296

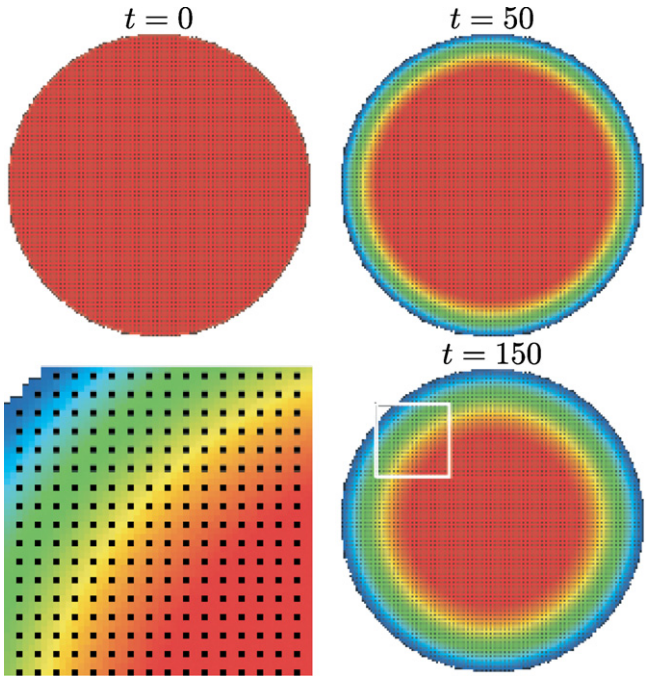

Fig. 2. Time evolution of the drug concentration inside a round drug capsule ($r_0 = 100$) with a periodic obstacle distribution ($C_{\text{obst}} = 1/9$). Shown is the drug concentration from low to high concentrations (denoted by colours ranging from blue to red, respectively). The concentration of drug is uniform inside the capsule at $t = 0$. The bottom left figure is a blow up of the indicated section in the $t = 150$ figure. (For interpretation of the references to colour in this figure legend, the reader is referred to the web version of the article.)

2.5. Round capsule with a periodic gel

We begin by constructing a simple periodic gel in order to compare our exact numerical results with empirical predictions and analytic results described in the previous section. We use a round 2D capsule constructed inside a 200 × 200 square lattice with a periodic obstacle distribution of concentration $C_{\text{obst}} = 1/9$ (see Fig. 2). The drug was loaded uniformly inside the matrix (i.e., the initial drug concentration was normalized at $C_0 = M_0/s$ for all sites that are not occupied by an obstacle, where s is the number of such sites). We calculate the time evolution of the population of non-interacting particles using Eq. (1) where t is given by the iteration step count, an integer.

The analytical function requires a value for the diffusion coefficient which we must obtain in order to compare the analytical profile with our exact numerical results. It is possible to fit the curve in order to extract the coefficient; however, there is a better way. The diffusion of a solute through an infinite lattice has been extensively studied by our group using another exact numerical approach (Mercier and Slater, 1999a,b). Using that technique, the scaled diffusivity for a particle in a periodic 2D square lattice of concentration C_{obst} was found to be given by:

$$D^* \simeq \frac{1 - \pi C_{\text{obst}} + (\pi^2/2)C_{\text{obst}}^2 + \dots}{1 - C_{\text{obst}}}. \tag{14}$$

This value for D^* is then used to calculate the release profile obtained by solving Eq. (10). The diffusion coefficient is

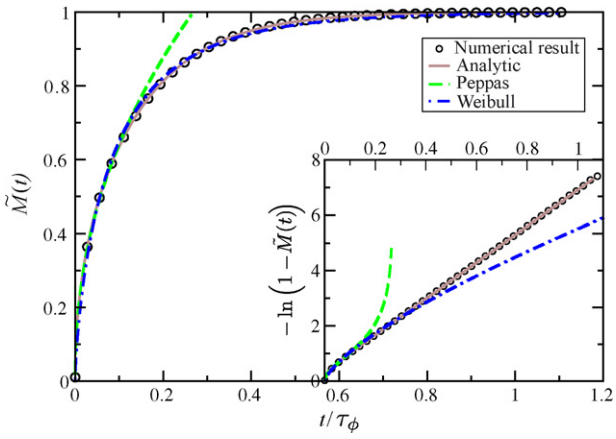

Fig. 3. Total drug release as a function of time for a round drug capsule of radius $r_0 = 100$ (see Fig. 2) with a periodic obstacle concentration $C_{\text{obst}} = 1/9$. The parameters of the different fits are (see text for definitions): Peppas, $t_\alpha/\tau_\phi = 0.25$, $\alpha = 0.46$; Weibull, $t_\beta/\tau_\phi = 0.092$, $\beta = 0.72$, $M(\infty) = M_0$ here since there are no traps; analytic, $C_0 = 1.0$, $D^* = 0.8008$, 5 terms in the series. The value for τ_ϕ was computed using $\phi = 0.999$ and was used to transform the data from both the enumeration and the analytic solution. The curves were then fitted on this transformed graph. The inset shows very good agreement of our data with the analytical solution by using a $-\ln(1 - \tilde{M}(t))$ y-axis transformation.

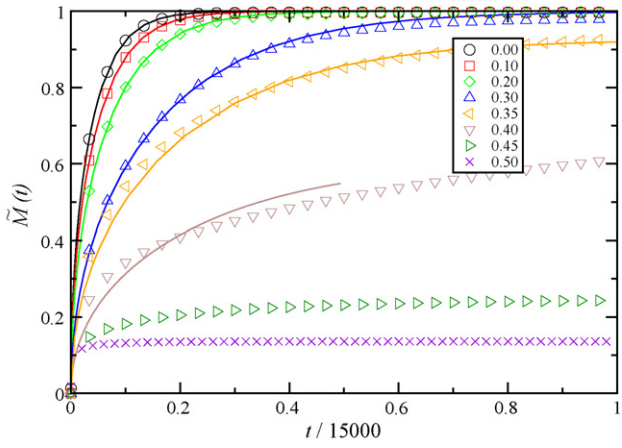

Fig. 4. Release profiles from circular random hydrogels with obstacle concentrations C_{obst} (shown in legend) with radius of $r_0 = 100$. There is a clear change in $\tilde{M}(t)$ as C_{obst} is increased. For the cases of $C_{\text{obst}} = 0.35, 0.40$, $M(\infty)/M_0$ were estimated to be 0.927 and 0.612 respectively by calculating the average amount of trapped particles. The solid lines are solutions to Eq. (10) with values of D^* obtained from Eq. (15) for shown obstacle concentrations and using $M(\infty)$ as the value of the effective initial load.

strictly used to compare Eq. (12) with results from our exact enumeration.

Fig. 3 shows a plot of the release profile as a function of time as well as the three fits mentioned in the previous sections. The inset shows another view of the same data. The Weibull fit is in good agreement with our release profile up to $\tilde{M}(t) \simeq 0.9$ and the Peppas fit is valid up to $\tilde{M}(t) \simeq 0.65$ The values obtained for the fitting exponents α and β are consistent with findings made by Papadopoulou et al. (2006) for Fickian diffusion. The value of $D^* = 0.8008$, as obtained from Eq. (14) for $C_{\text{obst}} = 1/9$, is used to plot Eq. (12) in Fig. 3. The analytical solution is in remarkable agreement with our exact numerical results for the release rate. This indicates that periodic obstacles can indeed be replaced by a constant viscosity within the hydrogel.

This example is used as a benchmark to properly gauge the accuracy of our model. At first glance these empirical laws seem to limit our control of the release rate. However, it is important to keep in mind that they are based on idealized conditions (uniform distribution of drug and obstacles, etc.) and thus it is possible to change these characteristics and manipulate the diffusion process. In Section 3, we present a method for obtaining release profiles that are different from these standard release curves in order to systematically control the drug release.

2.6. Round capsule with a random gel

The characteristics of drug release are strongly influenced by the behaviour of drugs which linger inside the hydrogel (e.g., slowly decaying tail on the drug release curves for long times). This behaviour is affected by the obstacle configuration and density. We now study the effects of altering the obstacle properties using a round capsule constructed inside a 200×200 square. The obstacles are placed randomly inside the round matrix and the drug is distributed uniformly on the remaining empty sites. The release curves are shown in Fig. 4 for varying obstacle concentrations. The solid lines correspond to solutions of Eq. (10). Again, we can obtain the scaled diffusivity from Mercier et al. (Mercier and Slater, 1999a,b) for 2D square lattices with randomly placed obstacles with concentration below percolation:

$$D^* \simeq 1 - (\pi - 1)\mathcal{C}_{\text{obst}} - 0.8558\mathcal{C}_{\text{obst}}^2 + \ldots \tag{15}$$

The resulting curves are in remarkable agreement with our enumeration results in the limit of low obstacle concentrations, $C_{\text{obst}} < 20\%$.

Due to the finite sizes of our hydrogels, the drug molecules will undergo anomalous diffusion for a certain portion of the release profile (except at $C_{\text{obst}} = 0$) before making a transition to normal diffusion. This is a well documented phenomenon and corresponds to a transition from anomalous diffusion to normal (or Fickian) diffusion which occurs after the molecules have travelled a certain cross-over length (or time) (Peppas, 1985; Chelminiak et al., 2005; Bonny and Leuenberger, 1993; Havlin and Ben-Avraham, 2002; Majid et al., 1984; Saxton, 1994). This cross-over length becomes larger as C_{obst} is increased until it is on the order of the size of our system (the cross-over length diverges at $\mathcal{C}^*_{\text{obst}}$). At this point, anomalous diffusion is observed for all times in our enumerations. Drug escapes from connected and tortuous pathways with a large number of dead ends altering the shape of the release profile (Stauffer and Aharony, 1992). Discrepancies between analytical and enumeration profiles are due to the fact that the analytical theory assumes a homogeneous diffusion coefficient throughout the hydrogel although this is not the case. Our enumeration model makes no such assumption and performs exact calculations of escape for each drug molecule from every hydrogel configuration.

There is also an increasing percentage of drugs which remain trapped inside the hydrogel as the obstacle concentration is increased. This is seen on Fig. 4 for release curves from hydrogels of $\mathcal{C}_{\text{obst}} > 0.30$. These profiles attain a plateau value which is

not equal to unity. We have access to the exact number of trapped particles during an enumeration and we can set the value of M_0 to be rescaled as $M(\infty)/M_0$ in order to compare the enumeration results with the analytical solution (Eq. (12) is used for the solid line fits in Fig. 4). As seen, the analytical theory breaks down in the near percolation limit. It is also interesting to note that the drug release rate can also be higher than anticipated. This can be seen on the release profile associated with an obstacle concentration $C_{obst} = 0.35$ where the initial release occurs at a faster rate than predicted by the analytical theory (see Eq. (4)). This is due to the creation of small drug "reservoirs" near the outer surface of the hydrogel which contributes an outward biasing effect.

This anomalous to normal diffusion transition has direct implications in controlling the release profile. These results suggest that high obstacle concentrations may favour slow, more constant release rate and that linear release could occur in a specific case of a power law regime (i.e., case II transport (Enscore et al., 1977)) of anomalous diffusion. In search of such a constant drug release profile, we will study the effects of systematically varying obstacle concentrations as a function of position. We will also compare drug release profiles from hydrogels with drug loaded uniformly versus hydrogels with discrete drug reservoirs. This will be shown in Section 4.

3. Genetic optimization methodology

3.1. Gel structure

Determining optimal obstacle density and placement is a daunting task considering the large number of degrees of freedom, therefore we limit ourselves to the simplest experimental case and search for structures which may be tested in the laboratory. Should any symmetry or pattern be observed in the course of our optimization such as onion structures (i.e., rings of varying obstacle densities), layers, or reservoirs we will use it to our advantage. Note that since we use a discretized version of the physical system and work on a 2D lattice, there is a finite number of spatial locations for the obstacles and solute particles. Finally, we restrict our examination to the low density drug limit where drug–drug interactions are negligible. In fact, there does not seem to be a significant change in the drug release profile from non-interacting particles compared to particles with hard-core excluded volume interactions (Bunde et al., 1985).

3.2. Fitness parameter

Finding a good fitness parameter is a critical factor for any optimization process. Our algorithm needs to identify the hydrogel/drug configurations which produce a targeted release profile using a simple quantitative test. Since we are aiming to produce constant release rates (over specified time intervals) we compute the following fitness parameter (see Fig. 5 for schematic illustration),

$$F = (1 - \gamma)\Delta\dot{M} - \gamma\langle\dot{M}\rangle. \tag{16}$$

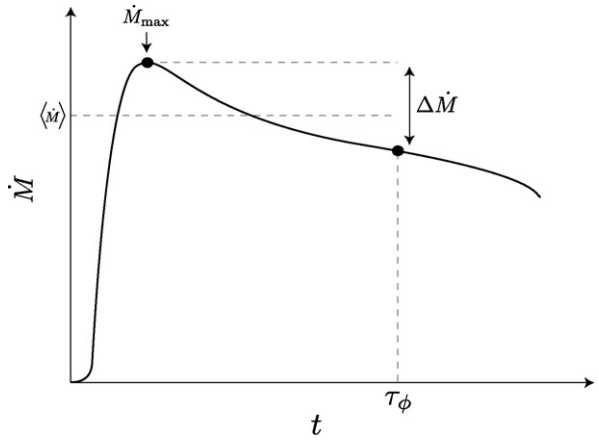

Fig. 5. Schematic illustration showing the parameters used to calculate the fitness parameter, F, in Eq. (16). This is an idealized drug release rate profile, $\dot{M}(t)$.

In this equation, $\Delta\dot{M} = \dot{M}_{max} - \dot{M}(\tau_\phi)$ is the maximum value of the rate of drug release from our simulated hydrogel minus the value of the release rate at some upper time τ_ϕ (smaller values of $\Delta\dot{M}$ indicate a more constant rate of release over that period of time). $\langle\dot{M}\rangle$ is the average rate of release during this time interval. This fitness parameter thus measures the linearity of the drug release by minimizing the slope of the rate of release curve starting from its maximal peak value while increasing the average rate. The value γ is an adjustment parameter which favours either minimizing the slope or maximizing the mean release rate. Adjusting this rate permits the creation of interesting hydrogel structures which are not shown in this article (i.e., γ is set to 0 except for Section 4.3 where it is set to 0.9).

It is important to note that an inherent lag time often exists at the beginning of the release process which must be neglected in order to obtain our fit (see Fig. 5). This lag time is a transient effect due to the arrival of the effective drug "wave front" and it is related to the geometry of the system (Barrer, 1953). This explains why we strictly look at the "post-peak" release process.

Our algorithm begins by initializing our first generation and calculating the fitness parameter, F, for each individual. Each generation is built using genetic characteristics from the best parents of the previous generation following the rules of the algorithm outlined in Section 3.3. In principle, it is possible to select an appropriate fitness parameter in order to achieve any desired functional form for the release profile, $M(t)$.

As an example consider a circular random hydrogel constructed inside a 100×100 square matrix. Fitness parameter data were obtained from the simulation perfomed in Section 4.2. Further details on the specifics used to implement the genetic algorithm are given therein. This system serves as our typical example here. Fig. 6 shows that our fitness parameter converges with increasing numbers of generations. The fitness parameter, F, is shown as a function of the generation number (ζ) for the three best candidates. In this example, the fitness parameter decreases sharply as a function of ζ until a cutoff generation $\zeta^* \simeq 10$. This has an important significance when determining the optimal number of generations needed to equilibrate each system. The fitness parameter decreases roughly as

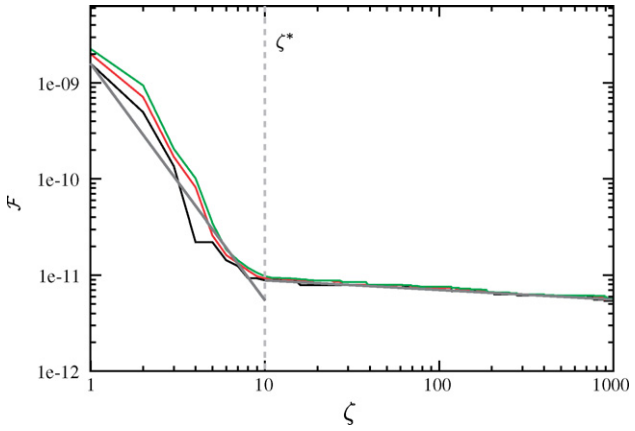

Fig. 6. Profiles of the fitness parameter, F, as a function of generation number, ζ, for the three best candidates during a genetic algorithm optimization. We use the system discussed in Section 4.2 for this demonstration although the general behaviour is similar for any system. The power law fits for the two regions are shown in grey and ζ^* in dashed grey. This type of data is a useful guide to gauge the required number of generations needed to attain sufficient convergence.

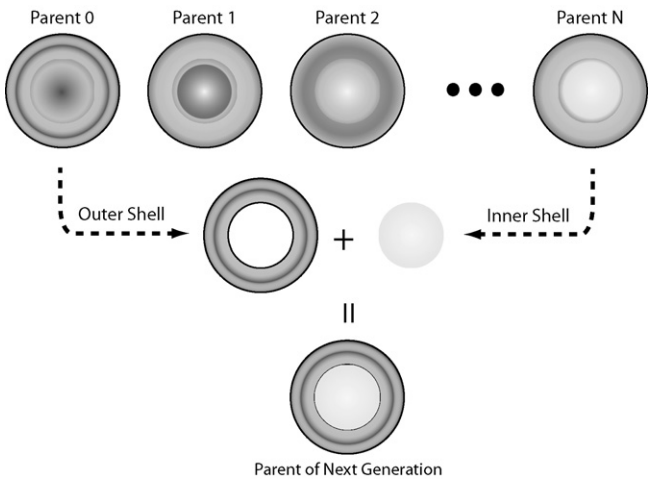

Fig. 7. Schematic illustration of a two ring cross-over from two randomly selected good parents to form an offspring in the next generation. The darker regions indicate higher concentrations of obstacles.

a power law for the region $\zeta < 10$ region: $F \simeq 1.6 \times 10^{-9}\zeta^{-2.5}$. For $\zeta \geq 10$, the fitness parameter approximately behaves like: $F \simeq 1.2 \times 10^{-11}\zeta^{-0.1}$ (shown in grey on the figure). This system has minimized the value of the fitness parameter very quickly at low values of ζ^*. Other systems usually follow a similar trend although they generally have higher values for ζ^*.

Fig. 6 also illustrates the learning mechanism of the algorithm. It shows various instances where a candidate acquires a favourable trait (i.e., sudden drop in effective fitness parameter) and passes those genetic characteristics to all others within a few generations.

3.3. Optimizing the initial obstacle distribution

We study the effects of "intelligently" placed obstacles and drug reservoirs using an extended Compact Genetic Algorithm (eCGA) (Sastry and Xiao, 2001). Genetic algorithms are able to quickly scan a large portion of phase space (i.e., the space of obstacle and drug placement locations) and thus efficiently find a minimum. They are a class of optimization algorithms which progress by acquiring successful traits from previous generations in order to quickly converge to a solution. In our case, an ensemble of drug capsules is first initialized based on a given basic design (e.g., an onion-like layering or chessboard pattern). Each drug capsule is then assigned a fitness parameter, F (see Section 3.2 for details). This parameter allows one to rank the capsules according to their ability to produce the desired output (e.g., a constant rate of escape). The entire ensemble (first generation) is then analyzed and ranked according to the fitness parameter. Once the best hydrogels are found, usually 10% are kept for the next generation (elitism) and a new generation of offspring is created using specific characteristics inherited from these "parents".We use three genetic mechanisms to construct our subsequent generations (there are many more genetic mechanisms but these will suffice for our proof of principle study). First, using a cross-over technique, we take the configuration of a predetermined section (e.g., ring-like structure) of a randomly selected parent and couple this with various other (ring-like) sections from other randomly selected parents. We combine these traits to generate the next generation (Fig. 7 illustrates such a cross-over for a circular drug capsule comprised of two rings). The second technique involves another type of cross-over where a mother and a father each donate randomly selected parts of their configurations in a chessboard pattern to form unique offsprings. The former technique is useful for configurations that exhibit angular symmetry and the latter for those with Cartesian symmetry.

Thirdly, once a generation is formed, a certain percentage of mutations are introduced in these offsprings. There are three possible types of mutation. The algorithm randomly changes an obstacle for a void, it can create an obstacle from a void and it can also change the location of an obstacle (the relative probability for the mutation to be of one type is: 25%, 25%, and 50%, respectively). These mutations lead to a more thorough "scanning" of the phase-space by introducing configurations that may not be obtained through simple genetic recombinations.

The resulting offsprings are then ranked according to our fitness test and the entire process is repeated until a satisfactory candidate is found. As a caveat, note that although genetic algorithms are very efficient at locating local minima in phase space there is no way to tell if we have reached the global minimum. In our simulations, we try to minimize the chance of being trapped in a local minimum by using a large number of generations and a relatively large percentage of mutations ($\geq$2% per generation).

3.4. Optimizing the initial drug reservoir position

The position and number of drug reservoir(s) may also need to be optimized in order to achieve our desired release rates. For example, in Section 4.3, the drug matrix is divided into a chessboard pattern, some sections of the capsule would then be given a probability of being a drug reservoir. The algorithm

is free to optimally alter the number and placement of drug reservoirs within the matrix.

3.5. Computational details

Most of the computational work was performed on 15 dual-core UltraSPARC IV+ processors with 576 GB of shared memory (www.hpcvl.org). Each simulation is executed over an average of 12 h (depending on the size of the matrix, the total Monte Carlo time required to obtain sufficient drug release, and the number of generations). Individual analysis and smaller simulations not requiring combinatorial optimization is performed on a 3.2 GHz P4 processor with 2 GB of memory.

4. Results

4.1. Spherical geometry with continuous drug distribution

The genetic algorithm is initially applied to a uniformly loaded circular random hydrogel constructed inside a 100×100 square lattice with radius $r_0 = 50$. The optimization is performed on the release profile from the moment that $\dot{M}(t)$ reaches its maximal value (this occurs at $t = 1$ since the hydrogel is uniformly loaded and there is no lag time in the drug release) until $\phi = 0.50$ and the adjustment parameter, γ, is set to 0. There are 1000 genetic generations and each generation is composed of 300 specimen.

Each hydrogel capsule is divided into five rings of equal thickness. The genetic algorithm creates new capsules using rings from five fit parents in the previous generation and randomly combines them as discussed earlier. Once a new hydrogel is created, mutations are introduced on 2% of the sites using the previously discussed mutation scheme.

The obstacle configuration of the optimized hydrogel can be seen in Fig. 8a. The associated obstacle concentration as a function of radial position, r, can be seen in Fig. 8c. By carefully observing Fig. 8a and b, one can notice the formation of a solid obstacle boundary (or membrane) at $r \simeq 45$ except for one small hole visible in the third quadrant of the circle. This boundary was created by the genetic algorithm in order to curtail the initial large release rate due to the bulk of the drugs' location near the surface of the hydrogel. The hydrogel has been divided into two sections with different obstacle concentrations: $C_{\text{obst}} = 0.05$ in the first region while the second region has an increasing obstacle concentration. On average for the whole capsule, $C_{\text{obst}} = 0.10$. Another feature of interest is that the centre of the hydrogel was chosen to contain very few obstacles (conversely, a large drug concentration). This would seem to minimize the overall impact of the initial release rate peak associated with the high drug concentration near the outer boundary of the hydrogel by locating the bulk of the drug in the centre. The ideal hydrogel seems to be one which tends to push the membrane closer to the surface of the hydrogel. By systematically increasing the value of ζ (the number of generations), we observe that it is pushed towards the outer boundary (not shown).

Fig. 9 shows the cumulative release as a function of time for our optimized hydrogel (solid line) as well as a comparison

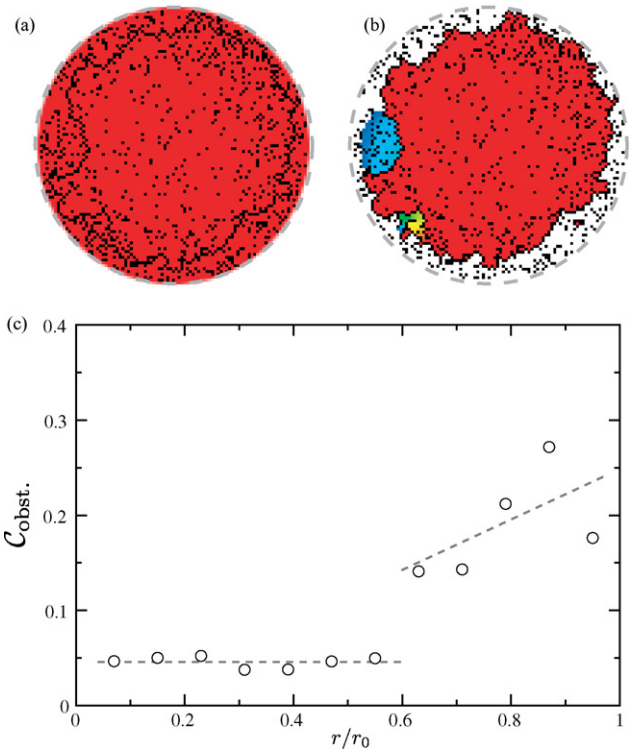

Fig. 8. (a) Optimal initial ($t = 0$) hydrogel configuration of a $r_0 = 50$ capsule; obstacles are in black. The dashed grey line represents the outer boundary of the hydrogel. (b) Retarding effect of the high obstacle concentration on the diffusion at $t = 1000$. There is also a very interesting visible feature—namely the formation of an obstacle barrier near the outer boundary of the hydrogel. The associated radial obstacle concentration profile is also shown in (c). The hydrogel has been separated into two distinct regions. The first region $0 < r < 0.6r_0$ has a very low obstacle concentration of $C_{\text{obst}} = 0.05$ and the second region has an increasing obstacle concentration.

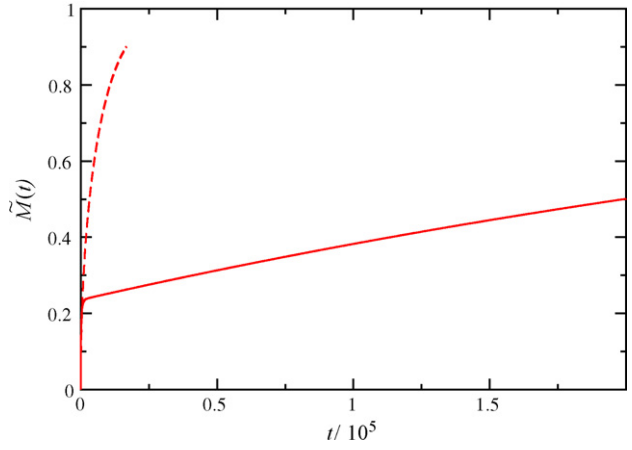

Fig. 9. Profiles of cumulative drug release as a function of time for the drug capsule shown in Fig. 8. This enumeration is performed until $\phi = 0.5$. There are 1000 genetic generations and each generation includes 300 specimen with a mutation percentage of 2%. The release is also compared to a control hydrogel with a uniform obstacle distribution equal to the average value of our optimized structure, $C_{\text{obst}} = 0.10$ (dashed line). The optimized release profile has two distinct regions. A quick initial release of drugs near the outer boundary followed by a linear release of drugs enclosed within the created obstacle boundary (porous membrane).

with a hydrogel of uniform obstacle concentration $C_{obst} = 0.10$ (dashed line). Since drugs initially occupy every non-obstacle site, drugs begin escaping the hydrogel as early as $t = 1$. This explains the steep initial slope observed for both hydrogels. However, once the drugs outside the bounded area observed in Fig. 8b have escaped, $M(t)$ in nearly lineary until $\phi \simeq 0.50$.

The circular geometry discussed in this section is a good demonstration of the usefulness of our genetic algorithm in optimizing drug release profiles. The genetic algorithm is able to find an optimized structure which produces a remarkably constant rate of release. The creation of the obstacle barrier seems to be a key component in controlling the release profile. This single hole membrane model has been extensively used in the past to obtain a constant drug release rate (Langer, 1998). It is quite interesting to note that the genetic algorithm was able to form a similar structure with no prior assumptions. The optimization appears to eliminate drugs from the boundary at the same time as creating this barrier. It would be logical to further test these hypotheses.

4.2. Spherical geometry with central reservoir

We re-examine the drug capsule geometry used in the previous section. However, the drug will now be initialized in a single central reservoir of radius $r = 10$. The single reservoir will curtail the effects of the strong initial drug release rate observed previously. The round capsule is constructed inside a 100×100 square with drugs evenly distributed in the reservoir. For the first generation, we initialize the drug capsule with five rings. Each ring has a width of 10 matrix sites with randomly chosen obstacle concentrations C_{obst} (each below the 2D percolation threshold). Our genetic algorithm is then applied.

There are a total of 1000 generations each one of which is composed of 300 specimen. Each specimen is simulated for a maximum of 200,000 time steps. Each generation is constructed using the first genetic technique discussed in Section 3.3 using a simple five ring swap (i.e., five chromosomes involved in the genetic optimization step) between five parents. Mutations are introduced after the cross-over at a rate of 2%.

The genetic algorithm is programmed to find the configuration of obstacles which would produce the most constant release rate in a specified range of drug release (from $\dot{M}_{max}$ up to $\phi = 0.50$ and $\gamma = 0$ here as well). The upper bound, $\phi = 0.50$ was chosen to be sufficiently high to control the bulk of the release profile without worrying about the tailing effect.

The resulting optimal configuration is shown in Fig. 10a and b shows the concentration of drugs in the hydrogel at $t = 5000$. The obstacle concentration profile has been divided into two sections (see Fig. 10c). The first section has a very low obstacle concentration of $C_{obst} = 0.08$ since it includes the drug reservoir (obstacles are allowed to enter the reservoir during genetic mutations). The second section has an average obstacle concentration of $C_{obst} = 0.38$ nearly at the percolation threshold. This section is suspected to be mainly responsible for having altered the shape of our release curve through the creation of another slow leaking membrane. The overall obstacle concentration is $C_{obst} = 0.32$. At least one ring with very high obstacle density

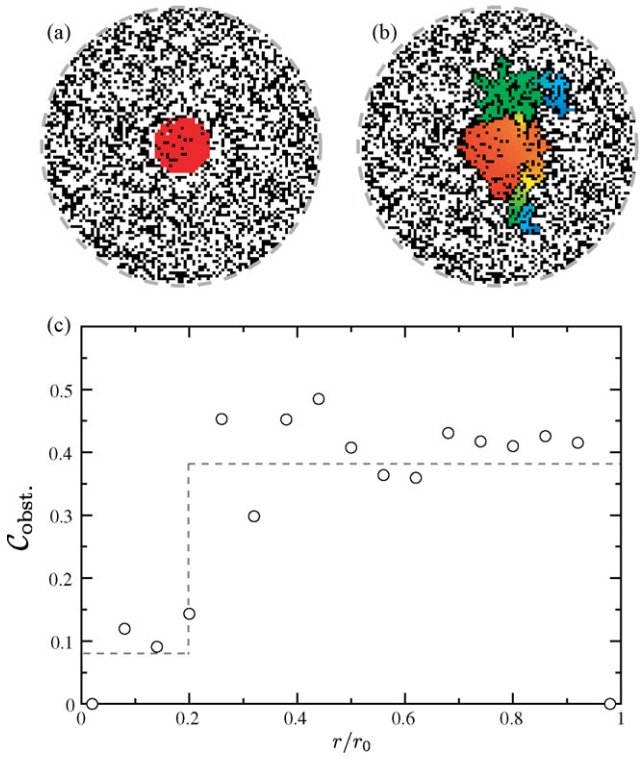

Fig. 10. (a) Optimal hydrogel configuration of a $r_0 = 50$ capsule (drug reservoir in red), obstacles in black and free space in white. The dashed grey line represents the outer boundary of the hydrogel. (b) Shows the retarding effect of the obstacles on the diffusion at $t = 5000$. The associated obstacle concentration profile is also shown in (c). The average obstacle concentration is indicated for two regions of the hydrogel. The reservoir with a width of 10 matrix sites has $C_{obst} = 0.08$ whereas the rest of the hydrogel is fairly uniform with $C_{obst} = 0.38$. The overall obstacle concentration is $C_{obst} = 0.32$. (For interpretation of the references to colour in this figure legend, the reader is referred to the web version of the article.)

has been observed in all specimens with this geometry and would appear to be a necessity to achieve controlled release rates.

Fig. 11 shows the escape rate and the cummulative amount of drug released as a function of time. The dashed line shows a comparison of our optimized results with a hydrogel of uniform obstacle concentration $C_{obst} = 0.32$ equal to the average obstacle concentration of our optimal structure (the rate curve was divided by 10 in order to compare its shape). The comparison hydrogel also has a central drug resevoir of radius $r_0 = 10$.

The release profile has been improved in terms of linearity from the one observed in our standard (dashed line). It is possible to quantify this by looking at the fitness parameters. Our standard has a fitness parameter $F = -2.9 \times 10^{-9}$. However, our optimal structure produces a much more constant release rate with $F = -5.4 \times 10^{-12}$. This optimization can be seen on the release rate curves (black). The optimized hydrogel shows a more constant release rate since the initial peak is less pronounced and the decay is much slower than the release rate from the standard.

It is quite remarkable that we are able to significantly alter the release profile by simply reorganizing the obstacle distribution around a central drug reservoir. This could lead to the development of spherical hydrogel matrices which produce a controlled drug release rate.

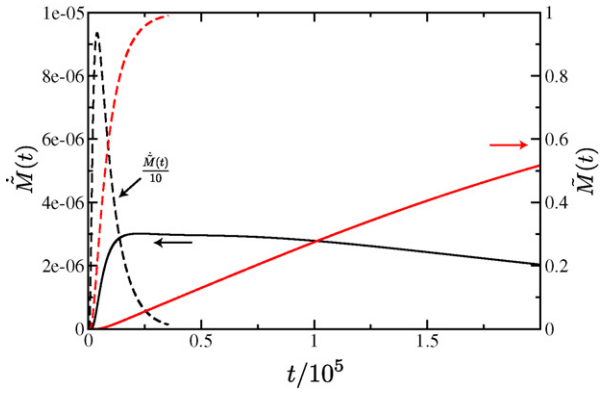

Fig. 11. Profiles of release rate, $\dot{\tilde{M}}(t)$, in black and total amount of released drugs as a function of time in red for the drug capsule shown in Fig. 10. This enumeration is performed until $\phi = 0.50$. There are 1000 genetic generations and each generation includes 300 specimens with a mutation percentage of 2%. The total release is also compared to a control hydrogel with isotropic obstacle distribution, $C_{\text{obst}} = 0.32$ (dashed line). The curve obtained from the comparison hydrogel was divided by 10. (For interpretation of the references to colour in this figure legend, the reader is referred to the web version of the article.)

4.3. Planar geometry with optimized reservoir distribution

We now examine a rectangular drug capsule which can be representative of a transdermal drug delivery system (Langer, 2004; Thomas and Finnin, 2004).

The 2D system presented here can be seen as a cross-sectional slice of such a system. This transdermal-type hydrogel allows us to use periodic boundary conditions: where drug particles leaving the system to the right are re-introduced on the left and vice versa. The unit cell of our periodic matrix measures 100×100 lattice sites and is now divided into grids measuring 10×10 sites. Each grid is initially given an obstacle concentration. We also allow the algorithm to choose the position and number of drug reservoir(s) in order to better control the drug release. The algorithm has a 20% chance of transforming a 10×10 obstacle grid into a drug reservoir during the initial creation of the hydrogel, $\zeta = 1$. These grids are now the chromosomes to be used by the eCGA.

We have incorporated the general trends observed in the previous sections directly into the initial conditions of our hydrogel in order to augment the efficiency of our optimization algorithm. In an attempt to reproduce the high obstacle concentration near the exit boundary, the lower boundary has been blocked with obstacles with the exception of 10 periodically placed holes in the unit cell. Note that during genetic mutations, these holes are free to change location or become blocked. The eCGA can now concentrate on finding optimal obstacle structures without having to invest reorganizing steps to form the previously observed high density layer of obstacles near the boundary.

This scheme allows for the optimization of both the obstacles and the placement of the drug reservoirs. The grid pattern allows for a greater number of chromosomes used in the optimization compared to the previous section. The eCGA also uses all three genetic recombination techniques discussed in Section 3.3. Each capsule is allowed to diffuse for 2×10^5 time steps. There are

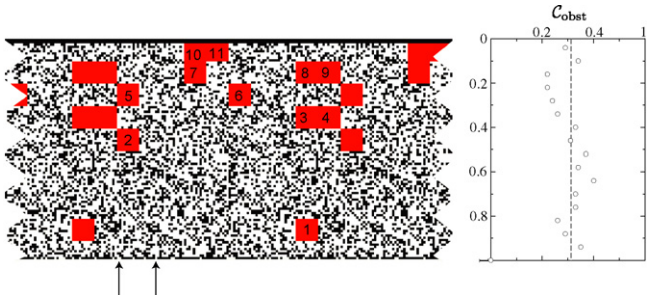

Fig. 12. Optimal drug delivery configuration of a 100×100 capsule with drug reservoirs in red, obstacles in black, and free space in white. Each drug reservoir is numbered and its contribution to the total release is shown on Fig. 13. There is a solid layer of obstacles on the top and bottom boundaries except for holes from which drugs can escape on the bottom (indicated by arrows in the unit cell). The obstacle concentration is shown to be quite constant inside the matrix ($C_{\text{obst}} \simeq 0.32$). (For interpretation of the references to colour in this figure legend, the reader is referred to the web version of the article.)

500 generations, each with 300 specimens and a mutation rate of 2%. The genetic algorithm optimizes the release profile up to $\phi = 0.5$ and here $\gamma = 0.9$.

The optimized hydrogel slice can be seen in Fig. 12. The unit cell is periodically repeated on both sides for illustrative purposes. It exhibits a number of interesting features. The obstacle concentration is fairly constant and near percolation throughout the drug matrix ($C_{\text{obst}} \simeq 0.32$). Remarkably, the eCGA has obstructed all of the holes on the boundary line (shown in green) except for two which were left open for drug release. Also, the density of drug reservoirs at each grid layer is increasing as the distance from the boundary increases.

Results obtained from this matrix are shown in Fig. 13. The drug release rate is rather linear for the range where 5% and 60% of the drug has escaped. Controlled release has therefore been obtained by adjusting the placement of obstacles and the initial position of drug.

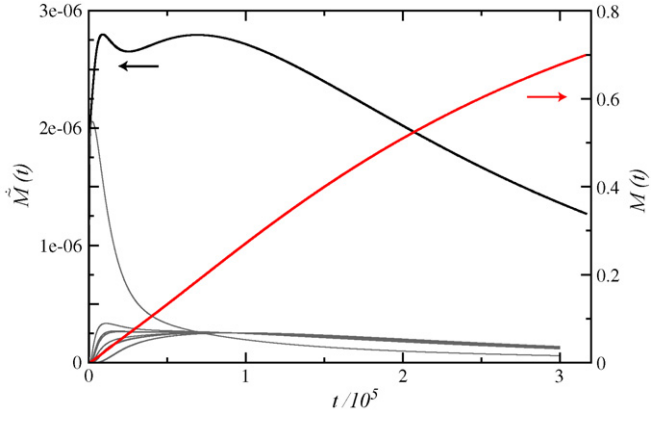

Fig. 13. Profiles of release rate (black) and total released drugs (red) as a function of time for the drug capsule shown in Fig. 12. This simulation ran for 3.3×10^5 time steps. There were 500 genetic generations and each generation comprised of 300 specimen. The genetic algorithm optimized the release profile up to $\phi = 0.5$. The contribution to the release rate by individual reservoirs is also shown in grey. (For interpretation of the references to colour in this figure legend, the reader is referred to the web version of the article.)

Since our drug particles are non-interacting, we are able to perform the simulation one reservoir at a time. This allows us to investigate the contribution to the total release from each reservoir. Fig. 13 shows the contribution of each reservoir to the total release curve (grey). The total release rate from this matrix is shown in black. The total release due to all the reservoirs is shown as the red curve.

These results are quite remarkable and testify to the power of this combinatorial approach. It is clear that controlled release can be achieved using our method and that it is a matter of carefully organizing the drug matrix itself. The algorithm finds a simple structure which consists of a concentration of obstacles near percolation and a carefully placed drug pyramid-like drug placement which yields a constant release rate. A similar structure could be implemented experimentally (at least qualitatively) to serve as the basis for a constant release drug platform.

5. Conclusion

In this article, we propose an exact enumeration model for drug diffusion which produces results that are in agreement with empirical fits and analytical data. Using this model, we can optimize the initial conditions of a given drug matrix in order to control the rate of drug release using a genetic algorithm. We use a simple fitting parameter in order to rank drug matrices according to their ability to produce our desired rate of release.

Each structure studied allowed us to gain valuable information pertaining to the behaviour of the release profile. We first showed that it is possible to favorably alter the release profile for the simple case of a round drug matrix with a central drug reservoir.

We can also control the release rate by using a rectangular transdermal-type drug matrix with horizontal periodic conditions. It is possible to control drug release by letting the eCGA optimize the location and number of drug reservoirs. The resulting matrix from this eCGA optimization was then used to show that it is possible to re-create a constant rate of drug release by changing the position and number of drug reservoirs. This allowed us to show the general characteristics drug matrices should have in order to produce a controlled rate of release.

To summarize we have demonstrated using a proof of principle study that we can systematically study the effects of drug matrix geometry on the behaviour of drug release. By beginning with a simple geometry with no immediately apparent structure and progressively varying the degrees of freedom of the system we were able to control the rate of drug release from our capsules. In particular we have shown that we can obtain an increasingly linear release rate in a reproducible manner with particular geometries that can provide impetus for the design of future drug delivery systems. The new optimization method introduced in this article can in principle be used for a wide range of drug delivery challenges.

Acknowledgments

The authors would like to thank M. Bertrand, E.C.J. Oliver, and F. Tessier for useful discussions. Computational analysis was supported by the High Performance Computing Virtual Laboratory (HPCVL). This work was financially supported by research grants from the Advanced Foods and Materials Network (AFMNet) and by the Natural Sciences and Engineering Research Council of Canada (NSERC) to GWS.

References

Amsden, B., 1998. Solute diffusion within hydrogels. Mechanisms and models. Macromolecules 31, 8382.

Barrer, R.M., 1953. A new approach to gas flow in capillary systems. J. Phys. Chem. 57, 35.

Bonny, J., Leuenberger, H., 1993. Matrix type controlled release systems. ii. Percolation effects in non-swellable matrices. Pharm. Acta Helv. 68, 25.

Bunde, A., Havlin, S., Nossal, R., Stanley, H., Weiss, G., 1985. On controlled diffusion-limited drug release from a leaky matrix. J. Chem. Phys. 83, 5909.

Chelminiak, P., Marsh, R.E., Tuszuhski, J.A., 2005. Asymptotic time dependence in the fractal pharmacokinetics of a two-compartment model. Phys. Rev. E 72, 031903.

Cohen, D.S., Erneux, T., 1998. Controlled drug release asymptotics. SIAM J. Appl. Math. 58, 1193.

Conaghey, O.M., Corish, J., Corrigan, O.I., 1998. The release of nicotine from a hydrogel containing ion exchange. Int. J. Pharm. 170, 215.

Crank, J., 1975. The Mathematics of Diffusion, second ed. Clarendon Press, Oxford.

Enscore, D.J., Hopfenberg, H.B., Stannett, V.T., 1977. Effect of particle size on the mechanism controlling *n*-hexane sorption in glassy polystyrene microspheres. Polymer 18, 793.

Hastedt, J.E., Wright, J.L., 1990. Diffusion in porous materials above the percolation threshold. Pharm. Res. 7, 893.

Havlin, S., Ben-Avraham, D., 2002. Diffusion in disordered media. Adv. Phys. 51, 187.

Kosmidis, K., Argyrakis, P., Macheras, P., 2003. Fractal kinetics in drug release from finite fractal matrices. J. Chem. Phys. 119, 6373.

Langer, R., 1998. Drug delivery and targetting. Nature 392, 5–10.

Langer, R., 2004. Transdermal drug delivery: past progress, current status, and future prospects. Adv. Drug Del. Rev. 56, 557–558.

Liang, H.-C., Chang, W.-H., Liang, H.-F., Lee, M.-H., Sung, H.-W., 2003. Crosslinking structures of gelatin hydrogels crosslinked with genipin or a water-soluble carbodiimide. J. Appl. Poly. Sci. 91, 4017.

Lin, C.-C., Metters, A.T., 2006. Hydrogels in controlled release formulations: network design and mathematical modeling. Adv. Drug. Del. Rev. 58, 1379–1408.

Liu, X., Nakamura, K., Lowman, A.M., 2003. Composite hydrogels for sustained release of therapeutic agents. Soft Mater. 1, 393.

Majid, I., Ben-Avraham, D., Havlin, S., Stanley, H.E., 1984. Exact-enumeration approach to random walks on percolation clusters in two dimensions. Phys. Rev. B 30, 1626.

Mallapragada, S., Colombo, P., Peppas, N., 1997. Crystal dissolution-controlled release systems. Ii. Metronidazole release from semicrystalline poly(vinyl alcohol) systems. J. Biomed. Mater. Res. 36, 125.

Mercier, J.-F., Slater, G.W., 1999a. Numerically exact diffusion coefficients for lattice systems with periodic boundary conditions. i. Theory. J. Chem. Phys. 110, 6050.

Mercier, J.-F., Slater, G.W., 1999b. Numerically exact diffusion coefficients for lattice systems with periodic boundary conditions. ii. Numerical approach and applications. J. Chem. Phys. 110, 6057.

Papadopoulou, V., Kosmidis, K., Vlachou, M., Macheras, P., 2006. On the use of the weibull function for the discernment of drug release mechanisms. Int. J. Pharm. 309, 44.

Peppas, N.A., 1985. Analysis of fickian and non-fickian drug release from polymers. Pharm. Acta Helv. 60, 110.

Peppas, N.A., Langer, R., 1994. New challenges in biomaterials. Science 263, 1715.

Reynolds, P.J., Stanley, H.E., Klein, W., 1980. Large-cell Monte Carlo renormalization group for percolation. Phys. Rev. B 21, 1223.

Saltzman, W.M., Olbricht, W.L., 2002. Building drug delivery into tissue engineering. Nat. Rev. 1, 177.

Sastry, K., Xiao, G., 2001. Cluster optimization using extended compact genetic algorithm. IlliGAL Report 2001016, p. 1.

Saxton, M.J., 1994. Anomalous diffusion due to obstacles: a Monte Carlo study. Biophys. J. 66, 394–401.

Siepmann, J., Peppas, N.A., 2001. Modeling of drug release from delivery systems based on hydroxypropyl methylcellulose (hpmc). Adv. Drug Del. Rev. 48, 139.

Stauffer, D., Aharony, A., 1992. Introduction to Percolation Theory. Taylor & Francis.

Thomas, B.J., Finnin, B.C., 2004. The transdermal revolution. Drug Discov. Today 9, 697–703.

Weibull, W., 1951. A statistical distribution function of wide applicability. J. Appl. Mech. 18, 293.